ISSN 1063-7729, Astronomy Reports, 2007, Vol. 51, No. 1, pp. 27–37. © Pleiades Publishing, Ltd., 2007.
Original Russian Text © E.E. Lekht, V.A. Munitsyn, V.V. Krasnov, 2007, published in Astronomicheskiĭ Zhurnal, 2007, Vol. 84, No. 1, pp. 30–40.

Chain-Type Structure in the H_2O Maser NGC 7538N

E. E. Lekht[1,2], V. A. Munitsyn[3], and V. V. Krasnov[4]

[1] *Instituto Nacional de Astrofísica, Óptica y Electrónica, Luis Enrique Erro No. 1, Apdo Postal 51 y 216, 72840 Tonantzintla, Puebla, México*

[2] *Sternberg Astronomical Institute, Universitetskiĭ pr, 13, Moscow, 119992 Russia*

[3] *Space Research Institute, Russian Academy of Sciences, Profsoyuznaya ul. 84/32, Moscow, 117997 Russia*

[4] *Pushchino Radio Astronomy Observatory, Astrospace Center of the Lebedev Institute of Physics, Russian Academy of Sciences, Pushchino, Moscow oblast, 142290 Russia*

Received December 20, 2005; in final form, July 7, 2006

Abstract—An analysis of the H_2O maser emission toward the source NGC 7538N, which is associated with an active star-forming region, is reported. The analysis is based on 24 years of monitoring in the 1.35-cm line using the the 22-m radio telescope of the Pushchino Radio Astronomy Observatory in 1981–2005 with a spectral resolution of 0.101 km/s. Individual spectral components have been isolated, and temporal drifts in their radial velocities found. From time to time, the drifts were accompanied by velocity jumps. This can be explained if there are chains consisting of clumps of material that are elongated in the radial direction toward the star and have a radial-velocity gradient. In 1982–2005, two maser activity cycles were observed, during which the chains were activated. We propose that shocks consecutively cross the chain elements and excite maser emission in them. The longest chain, at a radial velocity of −58 km/s, has not fewer than 15 links. For a shock velocity of 15 km/s, the chain step is estimated to be $\leq$1.5 AU. The chains could be located in a circumstellar disk with a width of $\leq 10^{15}$ cm. A structure in the form of a rotating nonuniform vortex with the rotation period of about 1.6 years has also been detected. The translational motion of the vortex may be a consequence of its orbital motion within the protoplanetary disk.

PACS numbers: 98.38.Er, 95.85.Bh, 98.35.Ac, 98.38.Dq
DOI: 10.1134/S1063772907010039

1. INTRODUCTION

NGC 7538 is an extended and intricate region in the Perseus Arm of the Galaxy at a distance of 2.8 kpc. It is associated, first and foremost, with a visible HII region. Approximately 2′ to the south, there is a compact cluster of three infrared sources, IRS 1–3. The region is also associated with a large complex of molecular clouds, which coincides with an extended HII region. This area is rich in dynamically developing star-forming regions, which are located in the core of a molecular-hydrogen cloud and are closely associated with high-velocity gas and ultracompact HII regions. NGC 7538 contains two H_2O maser sources (N and S) whose angular separation is 1′20″. The maser spots in NGC 7538N form two groups. The main, compact group coincides with an ultracompact HII region [1] and the infrared source IRS 1 [2]; it is located almost at the center of the molecular cloud, which emits an HCO^+ line at a radial velocity of −59.7 km/s.

A high-velocity molecular CO outflow, ionized gas outflow, and rotating disk around IRS 1 have been detected in this region. The core of the HII region contains multiple clumps with brightness temperatures of $\sim 1.5\times10^4$ K [3]. The continuum core consists of two components, northern and southern. The exciting star is probably at the center of the region. Ionized gas flows from the core of the HII region in the northern and southern directions.

According to CS-line observations [4], the velocity of the cloud core is about −57 km/s. The H_2O maser is nearly at the center of the HCO^+ molecular cloud, which has a radial velocity of −59.7 km/s [5]. Our 22-year monitoring of the H_2O maser has shown that the most probable position of the velocity centroid of the H_2O spectra is −57.5 km/s [6, 7], and the mean velocity for the entire emission interval in 1982–2003 is −58 km/s. Thus, the velocity of the central object in NGC 7538N can be estimated as $\sim$−58 to −57 km/s. This is significant for interpretation of the variability in the emission of some complex components (described in the literature as highly organized structures) of the H_2O maser in NGC 7538N.

The detection of highly organized structures, e.g., in the source S140, was based on an analysis of long-term H_2O maser monitoring data [8]. We detected two sequences of flares with velocity jumps: relay-race ignition and fading of subsources. MERLIN observations then revealed chain-type structures on various scales in this source [9]. One is about 60 AU in size and is associated with a protoplanetary disk around a massive star. Matveenko et al. [10] detected chains of compact components in two regions in Orion KL, which they associated with circular structures—protoplanetary rings. However, Shimoikura et al. [11] did not confirm these structures in Orion KL.

Chain-like structures were also found, e.g., in the envelope of the semi-regular variable RT Vir [12], where they represent fragmented filaments oriented radially toward the star.

This paper is devoted to a study of the structure of the H_2O maser-emission regions in NGC 7538N based on long-term monitoring data.

2. OBSERVATIONS AND SPECTRAL REDUCTION

Observations of the maser emission in the H_2O line at 1.35-cm were carried out toward the source IRS 1 of the intricate NGC 7538 complex ($\alpha_{1950} = 23^h11^m36.5^s$, $\delta_{1950} = 61°11'49''$) using the fully steerable, 22-m parabolic radio telescope of the Pushchino Radio Astronomy Observatory in 2003–2005. An antenna temperature of 1 K corresponds to a flux density of 25 Jy. The spectral analysis was performed by a 128-channel filter-bank spectrometer with a frequency resolution of 7.5 kHz (0.101 km/s in radial velocity at the 1.35-cm line). The frequency stabilization system of the first local oscillator provided a relative instability of $\pm 1.7 \times 10^{-8}$, which corresponds to ± 0.005 km/s for $\lambda = 1.35$ cm. In the observations with 0.1-km/s resolution, the maximum fluctuations in the line position did not exceed 0.1 of the spectral channel width. For intense (>50 Jy), not strongly blended lines, the accuracy of the measured radial velocity was better than 0.02–0.03 km/s. The instrumentation and its parameters were described in detail by Sorochenko et al. [13].

Figure 1 shows the H_2O spectra observed toward NGC 7538 in 2003–2005. The double arrow shows the vertical scale in Jansky. The horizontal axis plots the radial velocity relative to the Local Standard of Rest. The thin curves show the spectra toward the southern source (S), which is separated from NGC 7538N by 1′20″.

In our analysis, we also used all spectra from our monitoring data measured before 2003 [6, 7]. We can see from Fig. 1 that the southern source was the most active in 2003–2005. A considerable increase in its emission began at the end of 1999 [7], which was especially pronounced at velocities from −58 to −54 km/s and from −51 to −49 km/s. However, at velocities from −61.5 to −57.5 km/s and from −50 to −46 km/s, emission was observed only from the northern source. We used the results of Kameya et al. [14], Comoretto et al. [15], and Migenes et al. [16] to identify velocity intervals in our entire monitoring interval (1982–2005) where the emission from source N was considerably stronger than the emission from source S.

The maser emission toward NGC 7538 has displayed two pronounced activity cycles separated by 1993–1995, when there was a deep minimum of the maser emission. Accordingly, we carried out our study for the two time intervals 1982–1992 and 1996–2005. We selected narrow intervals (2–3 km/s) near velocities of −60, −54, and −47 km/s for the first maser-activity cycle and near −60.5, −58, and −47 km/s for the second, in which the emission from the northern source considerably exceeded that from the southern source.

When identifying components, we took as a basis pronounced line peaks that repeated from spectrum to spectrum. These peaks served as a reference. We then used the line shape (which turned out to be very important in our technique) to determine the positions of other components in the spectrum. We traced their temporal evolution, i.e., recorded the beginning and end of the time when the object was in the active emission phase. We then fitted Gaussians and found their amplitudes and radial velocities. In most cases, we repeated this procedure several times to improve the parameters of the fitted Gaussians (analogous to the method of successive approximations). This reduction method enabled us to reduce the errors in the derived fluxes and radial velocities of the components.

Figures 2–5 present the results of separating out individual components in all the spectra for the first activity cycle of the water-vapor maser (1982–1992). The main components are numbered. The large circles show the positions of the flux peaks, with the fluxes in Jansky given. The times when there is an anti-correlation between the fluxes of two components are labeled "AC", with the component numbers given in parentheses. In some time intervals, the variations in the V_{LSR} values for the components are approximated with straight-line segments.

Figures 6–8 and, partly, Fig. 4 show the results of a similar analysis for the spectra of the second activity cycle of the H_2O maser emission. The notation is the same as in Figs. 2–5.

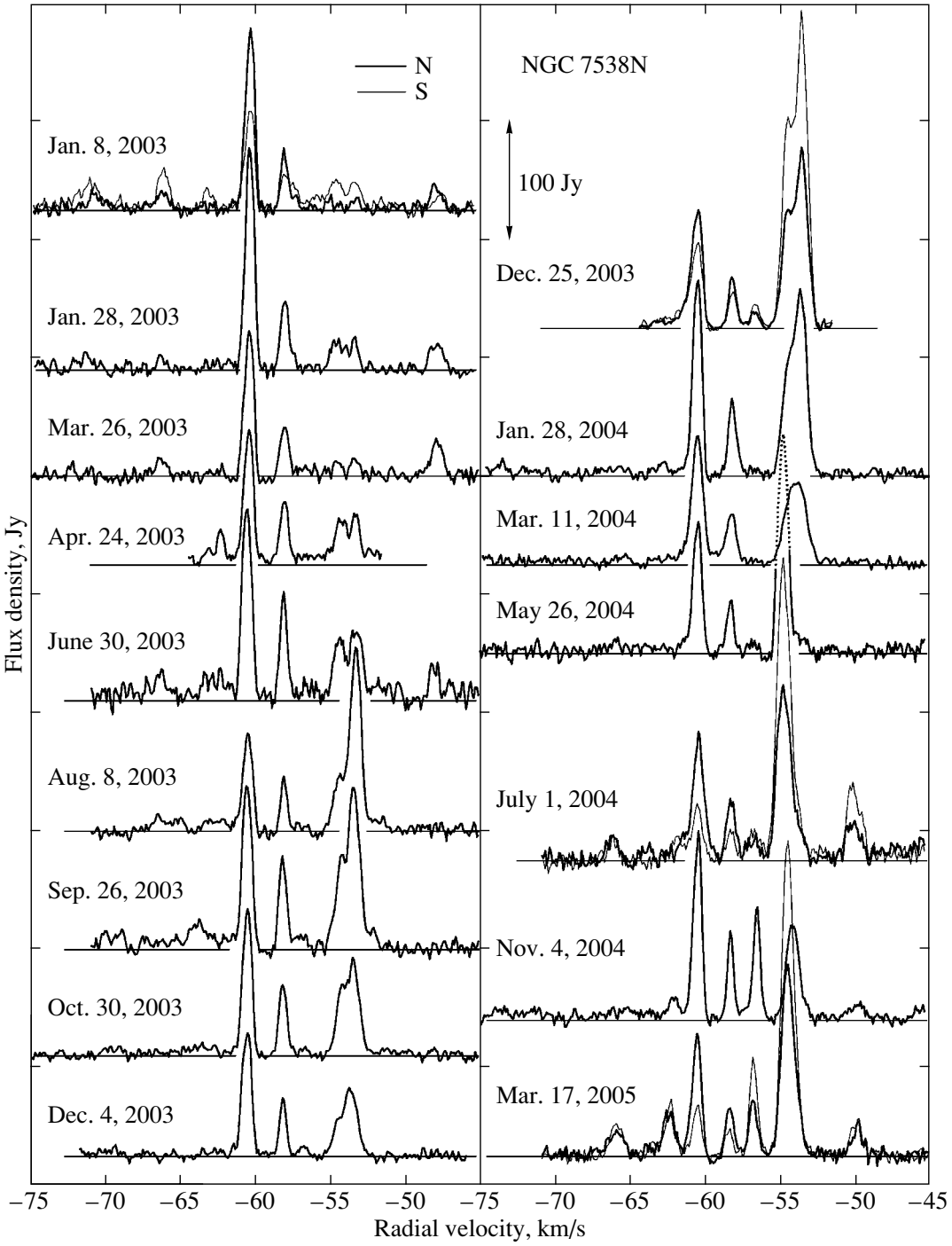

Fig. 1. H_2O maser emission spectra of NGC 7538N in 2003–2005. The double arrow shows the vertical scale. The thin curves show the spectra obtained toward source S.

In our analysis, we used only components with pronounced maxima; this enabled the accuracy in the radial velocities noted above. The remaining components are presented in the figures to portray the general pattern of the evolution of the maser emission in the intervals of flare activity.

3. ANALYSIS OF THE RESULTS

Isolation of individual components in three main groups of the H_2O spectra has shown time variations in the components' fluxes and radial velocities. We have detected four kinds of variability in V_{LSR}: (1) a slow, regular drift with a duration of 2–3 years; (2) fast

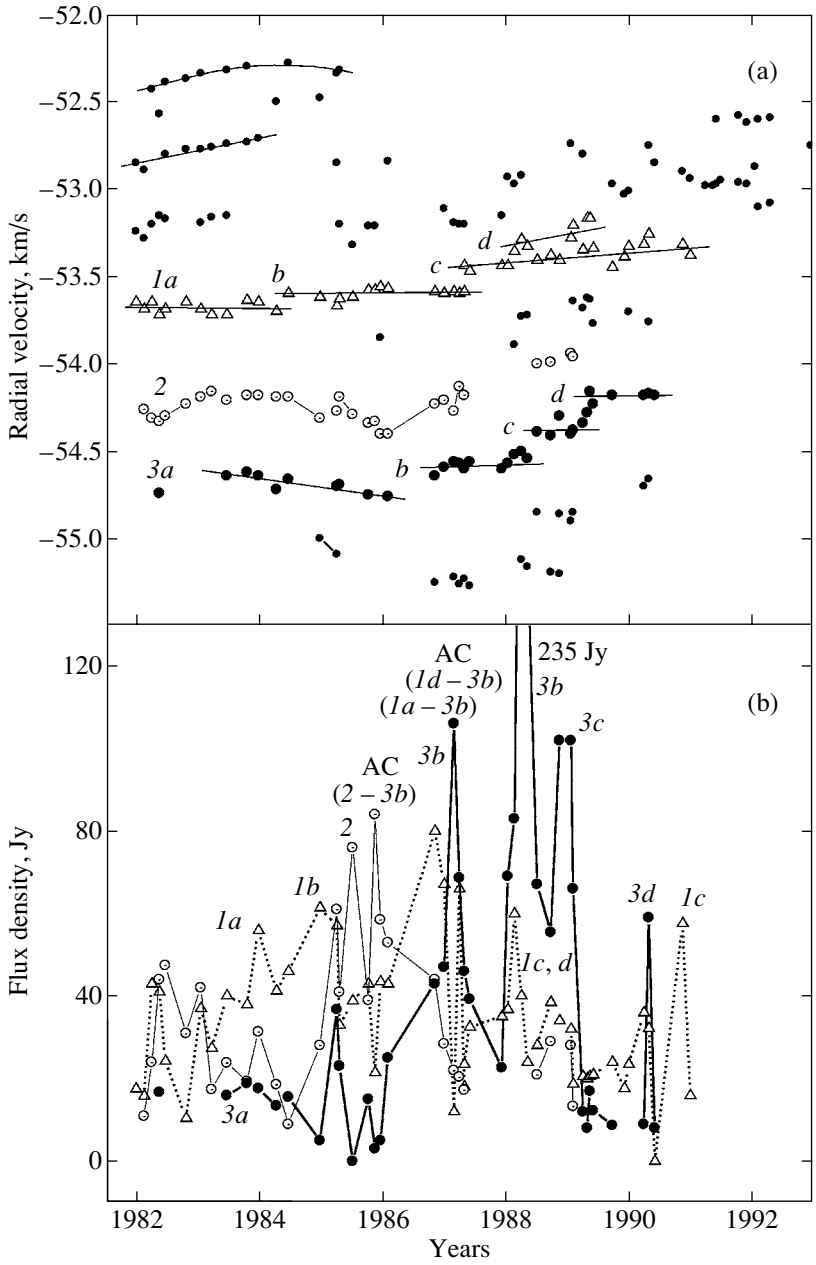

Fig. 2. Variations in the velocities and fluxes of individual H_2O spectral components during the first maser-activity cycle in the interval from −55.5 to −52 km/s. The strongest components are numbered (see text for details). The labels "AC" denote the times when the fluxes of the components whose numbers are given in parentheses are anti-correlated.

changes in the form of velocity jumps by 0.05 to 0.3 km/s; (3) mulitple successive jumps in one direction; (4) complex velocity variations. Most frequently there were superpositions of the first two kinds of drift.

What types of spot structures could correspond to certain kinds of drift? Jets of material with a velocity gradient could be responsible for the first kind of drift. Velocity jumps are possible when there are two clumps with similar V_{LSR} values located in very close proximity. If there are many clumps and they are arranged along some direction, a multiple-link chain structure is formed. This structure can be detected via monitoring if it is oriented in the radial direction toward the star or at some angle to this direction. Another condition is the presence of a radial-velocity gradient. The most important point in our technique is the flare activity of the maser.

Complicated drifts can occur when the structures discussed above have, e.g., some turbulent motions of their material.

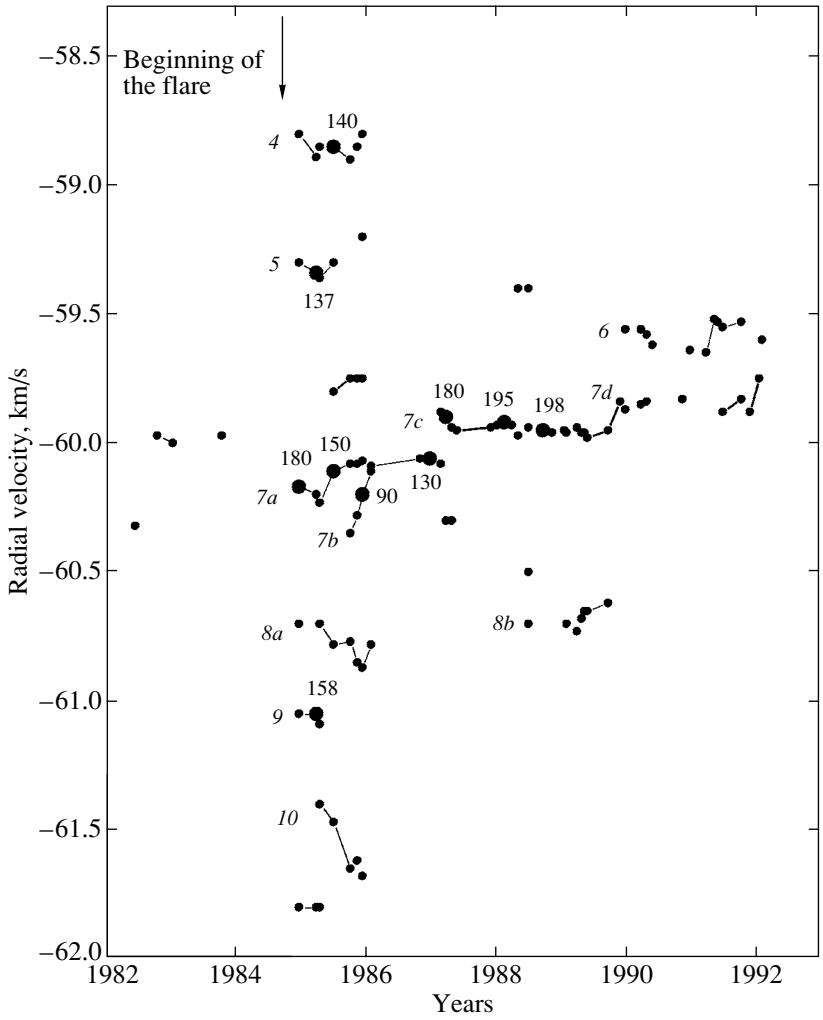

Fig. 3. Variations in the radial velocities of individual components in the interval -62 km/s $< V_{LSR} < -58$ km/s. The arrow shows the beginning of a strong maser flare. The large circles show the positions of emission peaks with the indicated flux densities in Jansky.

3.1. Correlations between the Fluxes of the H_2O Components

A study of variations in the emission fluxes of individual components enabled us to detect: (1) correlations of fluxes, either immediately at the positions of the emission peaks or with small time delay; (2) anti-correlations between fluxes of two components with similar radial velocities; (3) a mutual approach in V_{LSR} of two components at -60.12 and -60.35 km/s until their merging into a single component (end of 1985).

During the strong flare of 1984–1985, the delay between the emission peaks at velocities from -62 to -58 km/s was from six to ten months (Fig. 5). To estimate the thickness of the layer hosting the maser spots, we assumed a stellar-wind velocity of $\sim$500 km/s. In this case, the layer thickness is $\sim 10^{15}$ cm, which is considerably smaller than the overall size of the group of maser spots associated with IRS 1 (3×10^{16} cm) [13, 14].

In 1989–2000, maser activity was manifest at velocities from -47.5 to -45.5 km/s. Three main features were observed, at -46.1, -46.6, and -47.15 km/s (Figs. 4 and 5b). The emission peaks in these features were arranged in time precisely in this order, i.e., with decreasing velocity. The intervals between the peaks were one and two and a half months, respectively. All this testifies to the presence of an ordered structure in this group of maser spots. Their flux variations are probably correlated with those of the main features (-60 and -54.5 km/s), but with a delay of about ten months [6]. We observed no appreciable drift in V_{LSR}.

The detected anti-correlations took place between the fluxes of two emission features whose velocity

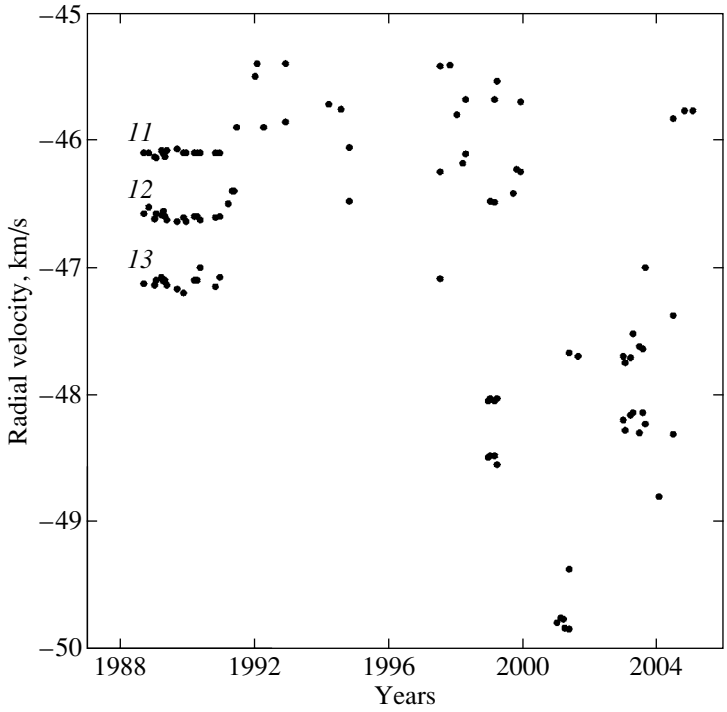

Fig. 4. Spectrum decomposition into individual components in the velocity interval from −45 to −50 km/s for the entire monitoring period.

difference did not exceed 1 km/s, i.e., it was within the thermal linewidth (Figs. 2 and 5). The anti-correlations were observed in two radial-velocity intervals: from −55 to −53 km/s and from −60.3 to −59.8 km/s. The time intervals for this phenomenon were from three to nine months. The fluxes grew and declined very rapidly. Such anti-correlations occurred only during the first H_2O-maser activity cycle, which was weaker than the second. Moreover, the focus of the maser activity in this interval was shifted toward higher radial velocities.

These properties of the emission could be related to the long-period variability of the H_2O maser in NGC 7538N; according to [7], its period is estimated as 13 years. However, the character of the velocity centroid variations [7] suggests that the period is much longer, and includes both maser-activity cycles (1982–1992 and 1996–2005). We also cannot rule out the possibility that the period for the long-term variability is related to either a bipolar outflow or the geometry of NGC 7538N, which is associated with the infrared source IRS 1.

3.2. Velocity Jumps

Temporal velocity jumps with magnitudes of 0.1–0.3 km/s took place for a large number of the emission features. In some multiple-link chains, the minimum velocity jumps were nearly as small as 0.05 km/s. The velocity jumps of different features were not correlated.

Alternation (in the form of jumps) of the emission of two features with velocity differences of 0.1–0.2 km/s took place mainly for features with low fluxes (e.g., features *1c* and *1d* in Fig. 2, features *6b* and *6c* in Fig. 6). Apparently, the emission of two components was anti-correlated here. The nature of this phenomenon consists in a competition between spatial modes of the radiation for pumping in a partially saturated maser.

A drift of another kind took place in components *4* and *6* (Fig. 6). The transition between the two velocity levels occurred over a fairly long time (1–1.5 years). We observed no correlation with the flux peaks as was observed in other multiple-link chains (see Section 3.4). Features *4b* and *4c* are probably elongated filaments with a velocity gradient.

3.3. Variability in the Maser Emission at −60 km/s

Throughout our monitoring the most intense emission was observed near a radial velocity of −60 km/s. The character of this variability was different in 1982–1992 and 1996–2005.

In the first activity cycle, we observed three jumps of V_{LSR} by 0.1–0.2 km/s, in the direction of increasing velocity (Figs. 3 and 5a). During the

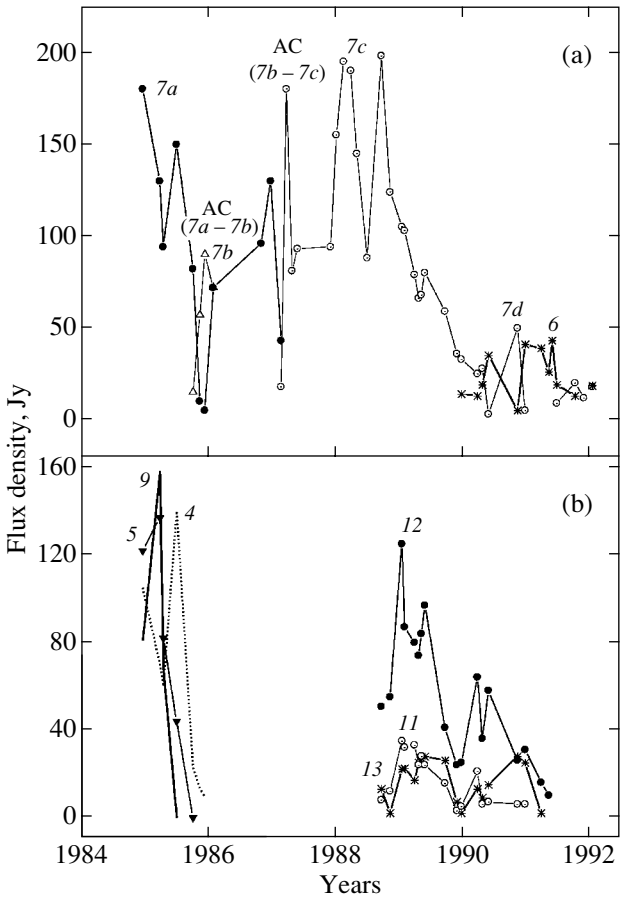

Fig. 5. Flux variations of emission features at (a) -60.5 km/s $< V_{LSR} < -59.5$ km/s, (b) -47.3 km/s $< V_{LSR} < -46$ km/s. The notation is the same as in Fig. 2.

first two jumps, the fluxes of the two features were anti-correlated; at the same time they alternated: one faded, while the other one flared. In general, the observed V_{LSR} drift of the strongest emission took place in jumps, but always toward higher velocities. This suggests the presence of separate fragments and of a velocity gradient in the regions responsible for the maser emission near -60 km/s.

In 1998–2003 we observed a complex drift in the radial velocity of the emission feature at -60 km/s. This can be represented as a uniform progressive drift superimposed with small cyclic variations in the velocity with an amplitude of $\sim$(0.05–0.08) km/s and a period of about 1.4–2.0 years. Another peculiarity is that the flux peaks fall on the same slope of the curve in each cycle (Fig. 7a).

We propose that this behavior could be produced by a rotating, turbulent vortex. The necessary condition for detecting the vortex rotation is the presence of inhomogeneities in the vortex. In addition to rotation, the vortex is moving with acceleration (deceleration) in the disk. The ambiguous character of the translational motion is due to uncertainty in the velocity of the system itself, i.e., of the central star. The velocity could be either slightly higher or slightly lower than -60 km/s (see the Introduction). In addition, the spot could be located at either the near or far side of the envelope. The translational motion of the vortex could be a consequence of orbital motion in the protoplanetary disk.

3.4. Multiple-Link Chains

Some components had several velocity jumps; as a rule, the jumps occurred in the same direction, toward higher or lower velocities. In many cases, this was due to the decline of a component and ignition of another at a nearby radial velocity. Such maser spots are most likely elongated in the radial direction with respect to the star, with each containin several clumps of material. A shock originating in the circumstellar envelope can move along this structure (chain), consecutively exciting maser emission in the clumps (chain links). A monotonic velocity variation from one link to another testifies to the presence of a radial-velocity gradient in the chain.

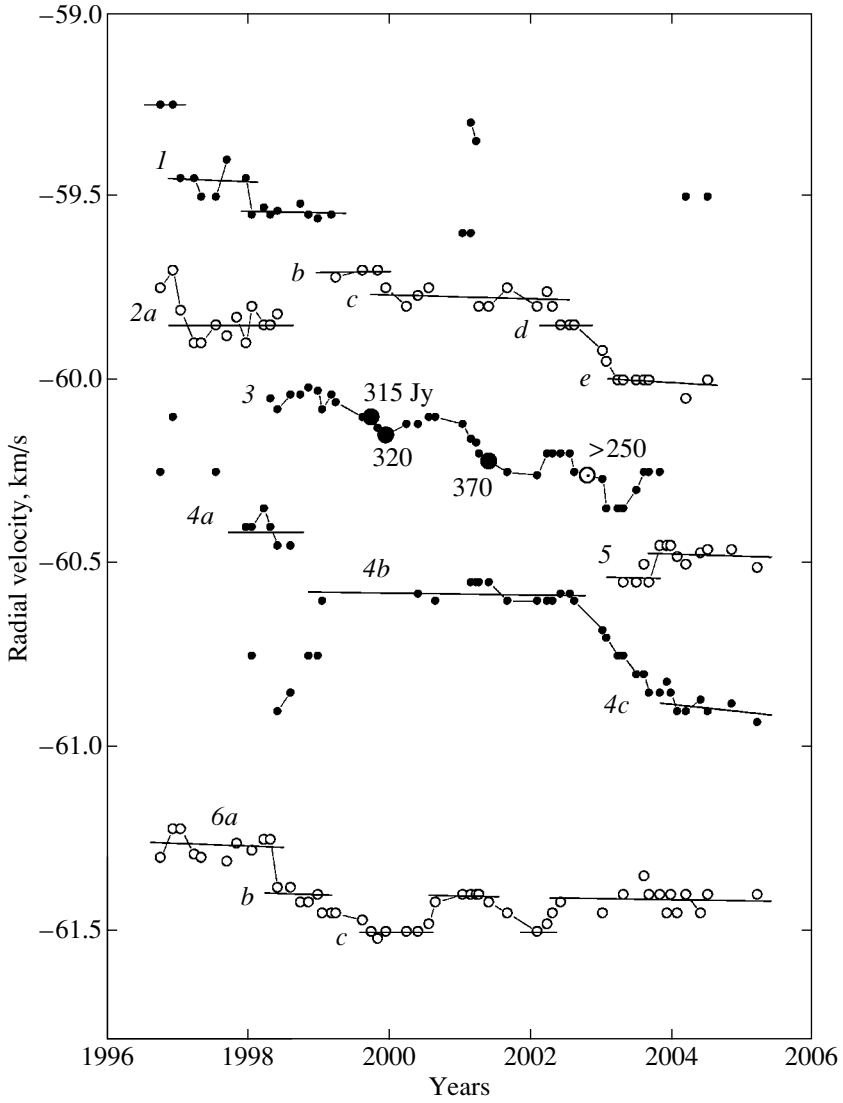

Fig. 6. Variations in the radial velocities of individual emission features in the second activity cycle of the H_2O maser emission at velocities from −62 to −59 km/s. The notation is the same as in Figs. 2 and 3.

We observed no chains only at velocities from −45 to −49 km/s. In the velocity interval from −58.5 to −57 km/s, two main chains (*A* and *B*) are observed (Fig. 8).

Chaim *A* has a very complex structure, consisting of at least 16 links. Beginning from the fifth link, we observed a consecutive decrease in the emission velocity. Each chain link has a counterpart flux peak. We propose that a shock that propagated radially outward excited maser emission in clumps of material whose velocities monotonically decreased. This is possible in the presence of a velocity gradient in this chain. We can assume that the shock propagation velocity in the chain is ≤15 km/s. Then, with the observed time of the active phase of the chain (links from 5 to 15) of 5 years, its length is 15 AU. The chain step, i.e., spacing between the centers of two adjacent links, can be estimated as ∼1.5 AU.

Chain *B* counts four links. From similar calculations, the chain length is ∼5 AU, and the link spacing is about 1.6 AU.

The fitted curve in Fig. 8b (thin dashed curve) shows the smoothed flux variations. This is more or less equivalent to the case of the passage of a shock along a homogeneous, elongated filament. The peak of the curve may correspond to the maximum in the optical depth of the medium hosting the filament (multiple-link chain). The curve itself probably reflects the water-vapor distribution in the envelope layer, which contains elongated chains consisting of separate clumps of material.

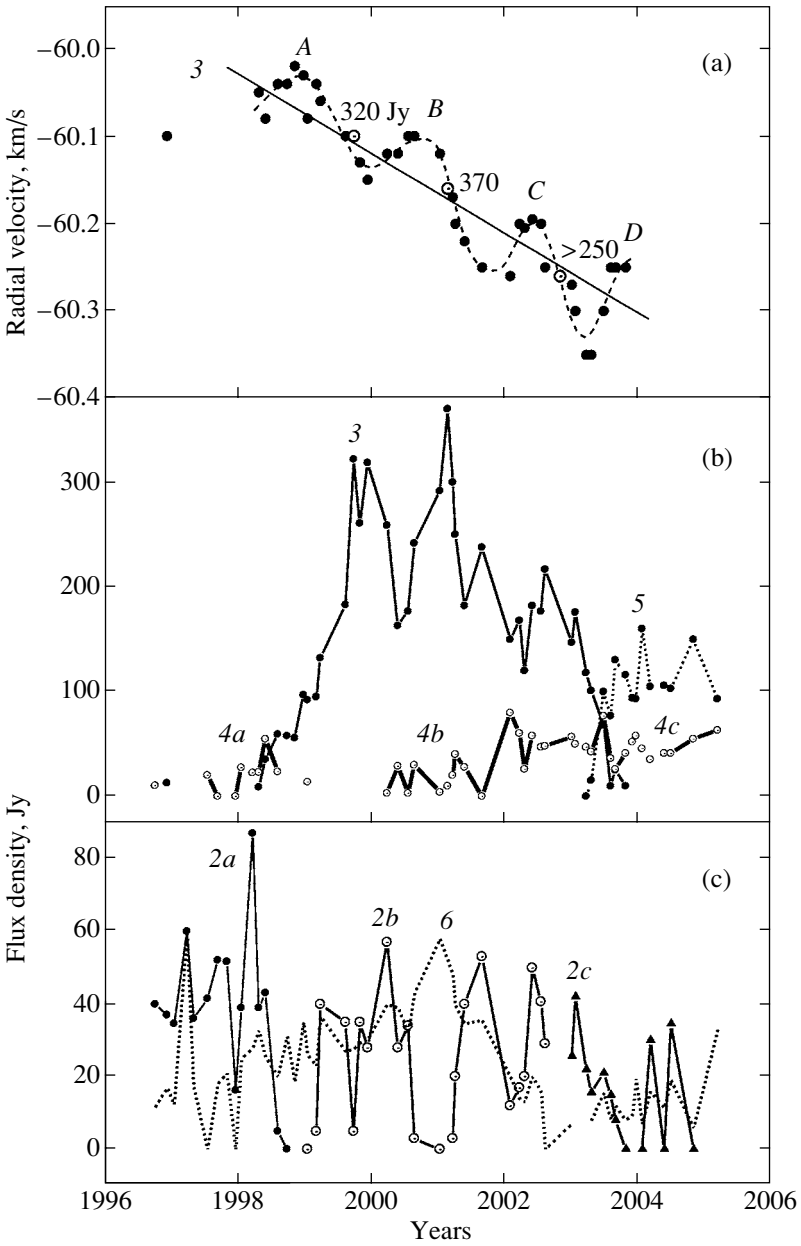

Fig. 7. Variability of the vortex-type structure (see text for details).

4. MAIN RESULTS

Below we list the most important results from our study of the variability of the H_2O maser emission of individual components based on our monitoring of NGC 7538 on the 22-m radio telescope of the Pushchino Radio Astronomy Observatory in 1982–2005.

(1) The H_2O spectra of NGC 7538N are complex. The strongest emission is concentrated in several narrow spectral intervals, which contain a large number of spectral features. This suggests fragmentation of the medium hosting the maser condensations. Most likely, most features in these spectral intervals form spatially compact groups.

(2) We have detected chain-type structures of maser spots, which are probably oriented radially (or close to radially) toward the protostar and have a radial-velocity gradient. The chain at −58 km/s contains no fewer than 15 links. The chain step is estimated to be $\leq$1.5 AU.

(3) The chains could be located in a circumstellar disk that is $\sim 10^{15}$ cm in size.

(4) We have detected a structure resembling a rotating, inhomogeneous vortex with a rotational period

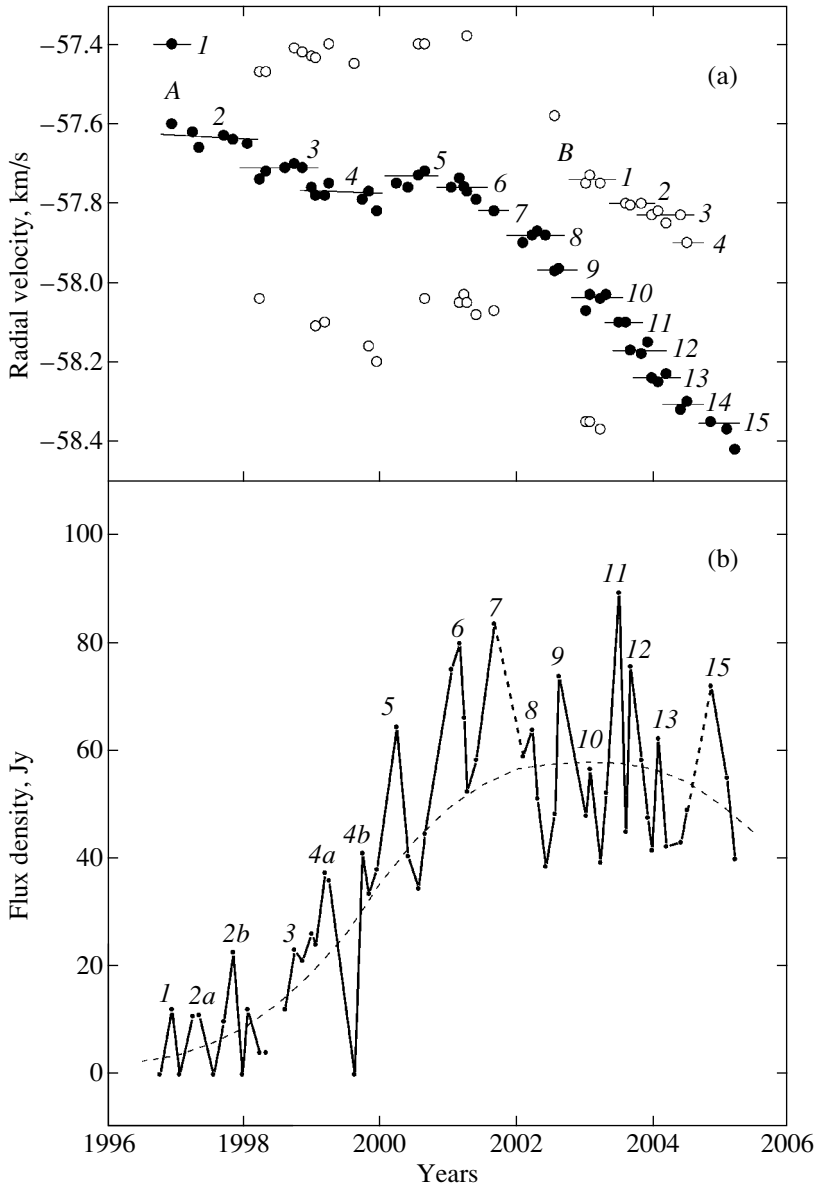

Fig. 8. Variations in V_{LSR} and the component fluxes in a compact group of features near −58 km/s. The chain elements and corresponding peak fluxes (for chain *A*) are numbered. The thin dashed curve shows the averaged smooth curve labeled as in Fig. 7.

of about 1.6 years. The regular drift of the vortex could be a consequence of its orbital motion in the protoplanetary disk.

ACKNOWLEDGMENTS

The RT-22 radio telescope facility is supported by the Ministry of Education and Science of the Russian Federation (registration number 01-10). The authors are grateful to the staff of Pushchino Radio Astronomy Observatory for help with the observations.

REFERENCES

1. B. Campbell and S. E. Persson, Astron. J. **95**, 1185 (1988).
2. C. G. Wynn-Williams, E. E. Beklin, and G. Neugebauer, Astrophys. J. **187**, 473 (1974).
3. R. A. Gaume, W. M. Goss, H. R. Dickel, et al., Astrophys. J. **438**, 776 (1995).
4. P. T. P. Ho, R. N. Martin, and A. H. Barrett, Astrophys. J. **246**, 761 (1981).
5. W. Batrla, P. Pratar, and L. E. Snyder, Astrophys. J. **330**, L67 (1988).
6. E. E. Lekht, V. A. Munitsyn, and A. M. Tolmachev, Astron. Zh. **80**, 909 (2003) [Astron. Rep. **47**, 838 (2003)].

7. E. E. Lekht, V. A. Munitsyn, and A. M. Tolmachev, Astron. Zh. **81**, 224 (2004) [Astron. Rep. **48**, 200 (2004)].
8. E. E. Lekht, S. F. Likhachev, V. S. Strel'nitskiĭ, and R. L. Sorochenko, Astron. Zh. **70**, 731 (1993) [Astron. Rep. **37**, 367 (1993)].
9. A. M. S. Richards, R. J. Cohen, M. Crocker, et al., Astron. Soc. Pac. Conf. Ser. **3**, 1 (1999).
10. L. I. Matveenko, P. D. Diamond, and D. A. Graham, Astron. Zh. **77**, 669 (2000) [Astron. Rep. **44**, 592 (2000)].
11. T. Shimoikura, H. Kobayashi, T. Omodaka, et al., Astrophys. J. **634**, 459 (2005).
12. E. E. Lekht, J. E. Mendoza-Torres, M. I. Pashchenko, and I. L. Berulis, Astron. Astrophys. **343**, 241 (1999).
13. R. L. Sorochenko, I. I. Berulis, V. A. Gusev, et al., Tr. Fiz. Inst. im. P.N. Lebedeva **159**, 50 (1985).
14. O. Kameya, K. I. Morita, R. Kawabe, and M. Ishiguro, Astrophys. J. **355**, 562 (1990).
15. G. Comoretto, F. Palagi, R. Cesaroni, et al., Astron. Astrophys., Supl. Ser. **84**, 179 (1990).
16. V. Migenes, S. Horiuchi, V. Slysh, et al., Astrophys. J., Suppl. Ser. **123**, 487 (1999).

Translated by G. Rudnitskii